Circular RNA CircCSPP1 Promotes the Occurrence and Development of Colon Cancer by Sponging miR-431 and Regulating the Expressions of ROCK1 and ZEB1

Jin Wang
Soochow University
Lei Zhou
Suzhou
Bingxin Chen
Soochow University Affiliated No 1 People\'s Hospital: First Affiliated Hospital of Soochow University
Zhuwen Yu
Soochow University
Jianglei Zhang
Soochow University
Zhe Zhang
Soochow University
Chenrui Hu
Soochow University
Yanjin Bai
Soochow University
Xiaokang Ruan
Soochow University
Shengjia Wang
Soochow University
Jun Ouyang
Soochow University
Airong Wu
Soochow University
Xin Zhao (zhaox@suda.edu.cn)
Suzhou University: Soochow University

Research Article

Keywords: circCSPP1, miR-431, Rho associated coiled-coil containing protein kinase 1, zinc finger E-box binding homeobox 1, colon cancer, cell cycle, epithelial-to-mesenchymal transition

Posted Date: December 28th, 2021

DOI: https://doi.org/10.21203/rs.3.rs-1199507/v1

Version of Record: A version of this preprint was published at Journal of Translational Medicine on January 31st, 2022. See the published version at https://doi.org/10.1186/s12967-022-03240-x.

Abstract

Colon cancer is a common malignant tumor of the digestive tract, and its incidence is ranked third among gastrointestinal tumors. The present study investigated the role of a novel circular RNA (circCSPP1) in colon cancer and explored the possible underlying molecular mechanisms. Bioinformatics analysis and reverse transcription-quantitative PCR were used to detect the expression levels of circCSPP1 in colon cancer specimens and cell lines. The effects of circCSPP1 on the behavior of colon cancer cells were investigated using CCK-8, Transwell and clonogenic assays. Bioinformatics analysis along with luciferase, fluorescence *in situ* hybridization and RNA pull-down assays were used to reveal the interaction between circCSPP1, microRNA (miR)-431, Rho associated coiled-coil containing protein kinase 1 (ROCK1) and zinc finger E-box binding homeobox 1 (ZEB1). It was found that circCSPP1 expression was significantly upregulated in colon cancer tissues and cell lines. The overexpression of circCSPP1 significantly promoted the proliferation, migration and invasion of colon cancer cells, whereas the silencing of circCSPP1 exerted opposite effects. Mechanistically, circCSPP1 was found to bind with miR-431. In addition, ROCK1 and ZEB1 were identified as the target genes of miR-431. Rescue experiments further confirmed the interaction between circCSPP1, miR-431, ROCK1 and ZEB1. Moreover, circCSPP1 promoted the expression levels of ROCK1, cyclin D1, cyclin-dependent kinase 4, ZEB1 and Snail, and lowered the E-cadherin expression level. Notably, circCSPP1 from SW620 cells was transferred to macrophages via exosomes and enhanced the colon cancer microenvironment. Taken together, the findings of the present study indicated that circCSPP1 may functions as a competing endogenous RNA in the progression of colon cancer by regulating the miR-431/ROCK1 and miR-431/ZEB1 signaling axes.

Introduction

Colon cancer is a common malignant tumor of the digestive tract, and its incidence is ranked third among gastrointestinal tumors (1). Over the past few decades, the rapid development of molecular biology has enriched the theory of colorectal cancer carcinogenesis (1–4). In addition, immense progress has been made in diagnostic and treatment strategies for colorectal cancer; the 5-year survival rate of patients with localized disease is 90.1% (5). However, following the metastasis of colorectal cancer to adjacent organs or lymph nodes, the 5-year survival rate of patients decreases to 69.2%. Of note, only 39% of patients with colorectal cancer are diagnosed at the localized stage of the disease, prior to metastasis (6, 7). Therefore, further in-depth investigations of the pathogenesis of colorectal cancer, as well as the identification of more effective early diagnostic and treatment strategies for colorectal cancer, are of utmost importance.

MicroRNAs (miRNAs/miRs) are small endogenous single-stranded RNA molecules composed of ~20 nucleotides, which act mostly on the 3'UTR of target mRNAs and either degrade or inhibit multiple transcripts (8, 9). Previous studies have demonstrated that miRNAs play a critical regulatory role in the initiation and progression of human cancers (10, 11).

Circular RNAs (circRNAs) are newly discovered non-coding RNAs with a covalently closed ring structure, which are widely found in a variety of cells (12–15). They are produced by the reverse splicing of

precursor mRNAs and are characterized by a stable structure, a conserved sequence and tissue specificity. Recent studies have indicated that circRNAs can act as miRNA sponges to inhibit the activity of targeted miRNAs (16, 17). In addition, circRNAs can regulate gene transcription by binding with RNA binding proteins, or can be translated to produce proteins (18). Thus, circRNAs play a vital role during the progression of tumors, and may provide a novel direction for tumor diagnosis and therapy (19, 20).

In the present study, the commonly differentially expressed circRNAs between colon cancer tissues and adjacent normal tissue in two datasets were screened with the aim of identifying novel molecular targets for the treatment of colon cancer. It was found that circCSPP1 was significantly upregulated in cancer tissues. In addition, the role of circCSPP1 in colon cancer was examined *in vitro* and *in vivo*.

Materials And Methods

Specimen collection. Cancer tissues and adjacent normal tissues were collected from 25 patients (14 male, 11 female), who diagnosed with colon cancer at the First Affiliated Hospital of Soochow University (Suzhou, China) (August, 2020 to July, 2021). These patients received no treatment before and age of them was range from 37 to 72 old. The tissues were stored in liquid nitrogen immediately after resection. The present study was approved by the Ethics Committee of the First Affiliated Hospital of Soochow University (No. FAHSU20200719) and written informed consent was obtained from each patient.

Gene Expression Omnibus (GEO) data analysis. The present study analyzed the GSE121895 and GSE126094 datasets from the GEO database. The expression levels in each group were normalized. The threshold value of differentially expressed genes was set at two of different multiples and $P<0.05$.

Cell culture and transfection. The human colonic epithelial cell line (HFC) was purchased from ScienCell Research Laboratories, Inc. Colon cancer cell lines, including SW620, SW480, LOVO, HCT116 and DLD-1 cells were obtained from the American Type Culture Collection (ATCC). THP-1 cells were also obtained from ATCC. The cells were maintained in DMEM (Thermo Fisher Scientific, Inc.) containing 10% FBS supplemented with 100 U/ml penicillin and 100 g/ml streptomycin (Beyotime Institute of Biotechnology) at 37˚C. When the cell density (SW620, LOVO) reached 50-70%, the cells were transfected with miR-431 mimics (20 nM), mimics control, circCSPP1 pcDNA3.1 overexpression plasmid (1 μg/μL) or circCSPP1 pLVX-IRES-Puro silencing plasmid (shRNA1 and shRNA2; 1 μg/μL) for 24 h using Lipofectamine® 3000 (Thermo Fisher Scientific, Inc.) according to the manufacturer's instructions. The miR-431 mimics, miR-control, circCSPP1 pcDNA3.1 overexpression plasmid, circCSPP1 pLVX-IRES-Puro silencing plasmids; Rho associated coiled-coil containing protein kinase 1 (ROCK1) and ZEB1 pLVX-IRES-Puro silencing plasmids were obtained from Shanghai Genepharma Co., Ltd. Phorbol-12-myristate-13-acetate (PMA), IL-4 and IL-13 were purchased from Sigma-Aldrich; Merck KGaA. The information of oligonucleotide was provided in Table 1.

Table 1
The information of oligonucleotide sequences

Gene	Sequence (5′-3′)
ROCK1 shRNA	sense: CACCGCATTTGGAGAAGTTCAATTGCGAACAATTGAACTTCTCCAAATGC
	antisense: AAAAGCATTTGGAGAAGTTCAATTGTTCGCAATTGAACTTCTCCAAATG
ZEB1 shRNA	sense: CACCGAGAGAGAGAGTTTGACAAGGCGAACCTTGTCAAACTCTCTCTCTC
	antisense: AAAAGAGAGAGAGAGTTTGACAAGGTTCGCCTTGTCAAACTCTCTCTCTC
circCSPP1 shRNA1	sense: CACCGCTCCAGACAATGAAACATCCCGAAGGATGTTTCATTGTCTGGAGC
circCSPP1 shRNA2	antisense: AAAAGCTCCAGACAATGAAACATCCTTCGGGATGTTTCATTGTCTGGAGC
shRNA control	sense: CACCGCTAATCAAGATACCTGTAGTCGAAACTACAGGTATCTTGATTAGC
	antisense: AAAAGCTAATCAAGATACCTGTAGTTTCGACTACAGGTATCTTGATTAGC
miR-431 mimic	sense: GATCCGTTCTCCGAACGTGTCACGTTTCAAGAGAACGTGACACGTTCGGAGAACTTTTTTG
mimic control	antisense: AATTCAAAAAAGTTCTCCGAACGTGTCACGTTCTCTTGAAACGTGACACGTTCGGAGAACG
miR-431 inhibitor	UGUCUUGCAGGCCGUCAUGCA
inhibitor control	UUCUCCGAACGUGUCACGUTT
	UGCAUGACGGCCUGCAAGACA
miR-324-5p mimic	UUCUCCGAACGUGUCACGUTT
miR-375 mimic	CGCAUCCCCUAGGGCAUUGGUG
	UUUGUUCGUUCGGCUCGCGUGA
miR-486-3p mimic	CGGGGCAGCUCAGUACAGGAU

Reverse transcription-quantitative PCR (RT-qPCR). TRIzol® reagent (Thermo Fisher Scientific, Inc.) was used to extract the RNA according to the manufacturer's protocol. The RNA was reverse transcribed into cDNA using a reverse transcription kit (Takara Bio, Inc.). The expression levels of miR-431, ROCK1 and zinc finger E-box binding homeobox 1 (ZEB1) were detected using a fluorescence quantitative PCR kit (Nanjing Jiancheng Bioengineering Inc.) in a BD FACSVerse™ (BD Biosciences). U6 and GAPDH were used as internal controls for miR-431 and mRNAs, respectively. Real-Time qPCRs were used three times: 2 minutes at 94°C, followed by 35 cycles (94°C for 30 s and 55°C for 45 s). The primers used were as follows: RT primer for miR-431, 5′-GTCGTATCCAGTGCAGGGTCCGAGGTGCACTGGATACGACACGUACU-3′; miR-431 forward, 5′-TGCGGUGUCUUGCAGGCCGUCAG-3′ and reverse, 5′-CCAGTGCAGGGTCCGAGGT-3′; U6 forward, 5′-CTCGCTTCGGCAGCACA-3′ and reverse, 5′-AACGCTTCACGAATTTGCGT-3′; ROCK1 forward, 5′-AACATGCTGCTGGATAAATCTGG-3′ and reverse, 5′-TGTATCACATCGTACCATGCCT-3′; ZEB1 forward, 5′-TTCTCACACTCTGGGTCTTATTCTC-3′ and reverse, 5′-CTTTTTCACTGTCTTCATCCTCTTC-3′; arginase-1

forward, 5’-AGACCACAGTTTGGCAATTGG-3’ and reverse, 5’-AGGAGAATCCTGGCACATCG-3’; IL-10 forward, 5’-AACCTGCCTAACATGCTTCG-3’ and reverse, 5’-GAGTTCACATGCGCCTTGAT-3’; circCSPP1 forward, 5'-CCATCCCATCAGTTCATCCT-3' and reverse, 5'-CCCTGCAAAAGGACTACAGG-3'; SMAD4 forward, 5'-GCTGCTGGAATTGGTGTTGA-3' and reverse, 5'-CTTCGTCTAGGAGCTGGAGG-3'; DAAM1 forward, 5'-TTCATTCATCTTTTGCTGTTTCCGA-3' and reverse, 5'-TTTTCTTCCTGGTCCTTTTTCTTGC-3'; CDK14 forward, 5'-GCACAGAGACCTGAAACCACAG-3' and reverse, 5'-AAAGATGCAACCTACTCCCCAC-3'; GAPDH forward, 5’-TCAAGAAGGTGGTGAAGCAGG-3’ and reverse, 5’-TCAAAGGTGGAGGAGTGGGT-3’. The data were quantified by using $2^{-\Delta\Delta t}$ method (21).

Cell Counting Kit-8 (CCK-8) assay. The SW620 or LOVO cells ($3x10^5$) were seeded in 96-well plates and cultured for 0, 24, 48 and 72 h. At each time point, the cells were incubated with 10 µl CCK-8 solution (Beyotime) at 37˚C for 4 h. The optical density was then measured at 450 nm as previously described (22).

Cell clonogenic assay. The cells ($5x10^3$) were suspended in DMEM containing 10% FBS, and then seeded into the plate. After 2 weeks of incubation at 37°C, the cells were fixed with 5 ml 4% paraformaldehyde for 15 min. The cells were then stained with Giemsa (Beyotime)for 30 min. The number of colonies was counted using a light microscope (200x; Nikon Corporation).

Transwell assay. The cells ($2x10^4$) were digested and cultured in a serum-free medium in the Transwell (BD) upper chamber with or without Matrigel (BD Biosciences). Subsequently, 600 µl complete medium (10% serum) were added to the lower chamber. After 24 h of incubation at 37°C, the cells in the lower chamber were fixed with 4% formaldehyde for 10 min at room temperature and stained with 0.1% crystal violet solution at room temperature for 10 min (Sigma-Aldrich; Merck KGaA). Finally, the migrated or invaded cells were photographed using a light microscope (200x)(23).

Fluorescence in situ hybridization (FISH) assay. Cy3-labeled circCSPP1 and FITC-labeled miR-431 probes (Biosense Technologies) were used to observe the co-localization of circCSPP1 and miR-431 in the cells. Hybridizations were performed according to the manufacturer’s instructions provided with the fluorescence *in situ* hybridization kit. The cell nuclei were stained with DAPI at room temperature for 20 min. Subsequently, images were visualized using a fluorescence microscope (200x) as previously described (24).

Luciferase assay. The luciferase assay was performed using the dual-luciferase reporting system psiCHECK (Thermo Fisher Scientific, Inc.). The wild-type (WT) or mutant-type (mut) sequences of circCSPP1, ROCK1 and ZEB1 were cloned into the psiCHECK2 plasmid. 293T cells (ATCC, $2x10^4$ cells/well) were cultured overnight in 24-well plates. The cells were transfected with the WT or mut reporter vector along with miR-431 mimics (10 nM) or mimics control (10 nM) using Lipofectamine® 3000 (Thermo Fisher Scientific, Inc.). Finally, the luciferase activity of cells was detected with a Dual-Luciferase Detection kit (Promega Corporation) after 48 h of transfection. The data were quantified by normalizing to Renilla luciferase activity.

RNA pull-down assay. Biotin labeled miR-431 and the control probes were synthesized by Sangon Biotech (Shanghai) Co., Ltd. Probe-coated beads were generated by co-incubation with streptavidin-coated beads (Thermo Fisher Scientific, Inc.) at 25˚C for 2 h. The SW620 and LOVO cells were collected, lysed and incubated with miR-431 probes overnight at 4˚C. Thereafter, the beads were eluted, and the complex was purified using TRIzol® reagent (Takara Biotechnology Co., Ltd.). The levels of circCSPP1, ROCK1 and ZEB1 were then analyzed using RT-qPCR.

RNA immunoprecipitation (RIP) assay. RIP assay was performed using the EZ-Magna RIP RNA-Binding Protein Immunoprecipitation kit (MilliporeSigma). Briefly, magnetic beads conjugated with negative control normal IgG (cat.no. AB21-KC, 1:5,000) or anti-Ago2 (cat.no. 03-110, 1:5,000) antibody (MilliporeSigma) were co-incubated with the cell lysates for 4 h at room temperature. To investigate the enrichment of the binding targets, the immunoprecipitated RNAs were extracted and subjected to RT-qPCR.

Western blot analysis. RIPA lysis buffer (Beyotime Institute of Biotechnology) was used to extract protein from the cells. The protein concentration was determined using the BCA kit (Nanjing Jiancheng Bioengineering Inc.) according to the manufacturer's instructions. Protein (40 µg) was then separated by using 10% SDS-PAGE, and transferred onto PVDF membranes (MilliporeSigma). The membranes were blocked in 5% skimmed milk for 1 h at room temperature followed by incubation with the following primary antibodies: ROCK1 (cat. no. #4035, 1:1,000, Cell Signaling Technology, Inc.), ZEB1 (cat.no. ab181451, 1:1,000, Abcam), cyclin D1 (cat. no. ab16663, 1:1,000, Abcam), cyclin-dependent kinase (CDK)4 (cat.no. 11026-1-AP, 1:1,000, ProteinTech Group, Inc.), p-CDK4 (1:1,000, Abcam), retinoblastoma (Rb; cat. no. ab181616, 1:1,000, Abcam), p-Rb (cat.no. ab184796, 1:1,000, Abcam), Snail (cat.no. ab216347, 1:1,000, Abcam), E-cadherin (E-cad; cat. no. 20874-1-AP, 1:1,000, ProteinTech Group, Inc.) and GAPDH (1:1500, cat. no. HRP-60004, ProteinTech Group, Inc.) at 4˚C overnight. The membranes were then incubated with HRP-labeled goat anti-rabbit secondary antibody (Abcam, cat. no. ab7090; 1:5,000) at room temperature for 1 h. Thereafter, an enhanced chemiluminescence kit (Thermo Fisher Scientific, Inc.) was used to detect protein expression.

Xenograft tumor model. Nude mice (n=24, 4-6 weeks old, 20-22 g) were obtained from the Animal center of Soochow University and randomly divided into four groups (shRNA2 ctrl, circCSPP1 shRNA2, pcDNA3.1 ctrl and pcDNA3.1-circCSPP1). All mice were housed in a SPF-grade animal room (temperature 18-22˚C; humidity 40-60%; light/dark cycle 12/12 h each day) and had free access to food and water. The subcutaneous injection of colon cancer cells was performed after 3 days of adaptive breeding. Each mouse was subcutaneously injected with $3x10^6$ colon cancer cells (100 µl in PBS). Tumor size was measured every 2 days, and the major axis (a) and minor axis (b) of the tumor were measured. The tumor volume was calculated using the following formula: $ab^2/2$. At the end of the experiment, the mice were sacrificed using a 40% volume/min CO_2 and the tumors were removed, photographed and weighed. The animal experiments were approved by the Ethics Committee of the First Affiliated Hospital of Soochow University (approval no. 20200917). The National Institutes of Health guide for the care and use of laboratory animals was strictly followed.

Isolation and characterization of exosomes. SW680 cells were cultured in DMEM supplemented with 10% FBS. Following 48 h of incubation at 37°C, the media were collected and centrifuged at 650 x g for 15 min, followed by 155,00 x g for 20 min at 4˚C (FBS was depleted of exosomes). The supernatants were then filtered (0.22 μm; MilliporeSigma) and centrifuged at 120,000 x g for 60 min at 4˚C. After washing with PBS, the exosome pellets were again centrifuged at 120,000 x g for 60 min at 4˚C. The quantity of exosomes was detected with BCA Protein Assay kit (Beyotime Institute of Biotechnology). Additionally, the particle size distribution of the exosomes was detected using NanoSight (Malvern Panalytical).

For observing the structure of the exosomes, transmission electron microscopy was used. Briefly, the exosomes were fixed with 2% paraformaldehyde and stained with 2% phosphotungstic acid (Beyotime) at 4°C for 2 min. The samples were then observed using a transmission electron microscope (Hitachi, Ltd.). In addition, fluorescent PKH67 dye (Thermo Fisher Scientific, Inc.) was used to label the exosomes at 4°C overnight and fluorescent Phalloidin dye (Thermo Fisher Scientific, Inc.) was used to label the cytoskeleton at room temperature for 2 h.

Cell cycle distribution analysis. SW620 or LOVO cells ($5x10^5$) were fixed using with 75% ethanol for 20 min on ice. Then, cells were permeabilized with 0.25% Triton X-100 and stained with PI/RNase (Sigma Aldrich). After 15 min of incubation at 4˚C, cells were analyzed using a flow cytometer (BD FACSAria III; BD Biosciences) and ModFit (version 3.0; Verity Software House, Inc.).

Statistical analysis. Three independent experiments were performed in each group. Statistical analysis was performed using GraphPad Prism software (GraphPad Software, Inc.). The measurement data are expressed as the mean ± standard deviation. The unpaired Student's t-test was used for comparisons between two groups, and One-way analysis of variance and Tukey's post hoc tests were used for comparisons between multiple groups (25). $P<0.05$ was considered to indicate a statistically significant difference.

Results

circCSPP1 is highly expressed in colon cancer. To explore novel molecular targets for the treatment of colon cancer, the differentially expressed circRNAs in cancer and adjacent normal tissues were first analyzed using two GEO datasets (GSE121895 and GSE126094) (Fig. 1A). Intersection analysis of the two omics data identified a total of 161 differentially expressed circRNAs (Fig. 1B). Further verification at the tissue level revealed that hsa_circ_0001806 (circCSPP1) was significantly upregulated in colon cancer (Fig. 1C and D). Consistently, compared with the HFC cells, the circCSPP1 level was found to be upregulated in colon cancer cells (Fig. 1E). In addition, circRNA circularization data indicated that circCSPP1 was spliced by exons 8-11 of the CSPP1 transcript, which was confirmed by Sanger sequencing (Fig. 1F).

Subsequently, the distribution of circCSPP1 in the cells was detected using FISH assay and RT-qPCR. The data revealed that circCSPP1 was mainly located in the cytoplasm (Fig. 1G and H). Compared with linear

RNA, circCSPP1 was more resistant to actinomycin or RNase R treatment (Fig. 1I and J). These data thus indicated that circCSPP1 had higher stability and a longer half-life.

Knockdown of circCSPP1 significantly inhibits the tumorigenesis of colon cancer. In order to investigate the role of circCSPP1 in colon cancer, cell proliferation, invasion and migration were detected. First, the expression of circCSPP1 was knocked down in colon cancer cells using shRNA1 and shRNA2. The results of RT-qPCR revealed that both these shRNAs effectively suppressed the level of circCSPP1 in the cells (Fig. 2A). In addition, the results of the CCK-8 assay demonstrated that the knockdown of circCSPP1 significantly inhibited the proliferation of colon cancer cells (Fig. 2B). Consistently, circCSPP1 knockdown notably decreased the colony-forming ability of the cells (Fig. 2C). Moreover, Transwell assay revealed that the knockdown of circCSPP1 inhibited the invasive and migratory ability of colon cancer cells (Fig. 2D and E). These data thus suggested that the knockdown of circCSPP1 significantly inhibited the progression of colon cancer.

circCSPP1 promotes colon cancer tumor growth and metastasis in vivo. With the purpose of confirming the biological function of circCSPP1 in colon cancer, an animal experiment was performed. The results of the animal experiment revealed that the overexpression of circCSPP1 significantly promoted tumor growth, whereas the knockdown of circCSPP1 inhibited tumor growth (Fig. 3A-D). Moreover, the metastasis of colon cancer *in vivo* was assessed. The results indicated that circCSPP1 knockdown notably decreased the metastasis of colon cancer, whereas circCSPP1 overexpression promoted metastasis (Fig. 3E and F). In addition, the level of circCSPP1 in tumor tissues was inhibited by circCSPP1 shRNA2, while it was upregulated by circCSPP1 (Fig. 3G). On the whole, these data indicated that circCSPP1 promoted colon cancer tumor growth and metastasis *in vivo*.

circCSPP1 sponges with miR-431 in colon cancer cells. To explore the potential target of circCSPP1, Circinteractome (https://circinteractome.irp.nia.nih.gov/) was used. A total of six miRNAs (miR-197, miR-324-5p, miR-375, miR-431, miR-324-5p and miR-486-3p) were predicted to be the candidate targets of circCSPP1 (Fig. S1A). Luciferase reporter assay was then used to screen the candidate binding miRNAs. The data revealed that the relative luciferase activities of the cells were notably inhibited by miR-431 mimics or miR-486-3p mimics (Fig. S1A). Based on these data, miR-431 was demonstrated to be the most likely candidate target. The binding site between circCSPP1 and miR-431 is presented in Fig. S1B. Subsequently, luciferase reporter assay confirmed that circCSPP1 was able to bind to miR-431 (Fig. S1C). In addition, the results of FISH assay revealed the co-localization of circCSPP1 with miR-431 in the cytoplasm of the cells (Fig. S1D). Moreover, RIP and RNA pull-down assays revealed that circCSPP1 could directly bind with miR-431 and RT-qPCR data suggested knockdown or overexpression of circCSPP1 did not affect the expression of miR-431 in cell (Fig. S1E, F and G). Thus, these data suggested that circCSPP1 sponged miR-431 in colon cancer cells.

ROCK1 is a target gene of miR-431 in colon cancer cells. TargetScan (http://www.targetscan.org/vert_72/), miRDB (http://www.mirdb.org/) and miRWalk (http://zmf.umm.uni-heidelberg.de/apps/zmf/mirwalk/micrornapredictedtarget.html) were then used to explore the target genes of miR-431 in colon cancer cells. The expression of several potential targets involved in cancer

development was assessed. Based on these three databases, ZEB1, SMAD4, disheveled associated activator of morphogenesis 1 (DAAM1), CDK14 and ROCK1 were predicted to be the candidate targets of miR-431 (Fig. S2A). ZEB1 and ROCK1 were found to be downregulated by miR-431 mimics (Fig. S2A). Among these genes, ROCK1 was first selected for further analysis due to its critical role in the progression of cancer (26).

RT-qPCR data then revealed that ROCK1 expression was notably upregulated in colon cancer tissues compared with adjacent normal tissues (Fig. S2B). The potential complementary pairing sequence between miR-431 and the 3′-UTR of ROCK1 is presented in Fig. S2C. In addition, luciferase reporter assay indicated that the luciferase activity of the cells carrying the WT ROCK1 3′-UTR was significantly reduced by miR-431 mimics (Fig. S2D). Consistently, the results of RIP and RNA pull-down assays revealed the direct interaction between miR-431 and ROCK1 (Fig. S2E and F). On the whole, these data confirmed that ROCK1 was a target gene of miR-431 in colon cancer cells.

Knockdown of ROCK1 reverses the tumor-promoting effects of circCSPP1. To further confirm the interaction among circCSPP1, miR-431 and ROCK1, rescue experiments were performed. The results of RT-qPCR revealed that the overexpression of circCSPP1 promoted ROCK1 expression, whereas this effect was reversed by transfection with miR-431 mimics (Fig. 4A). In addition, the data of CCK-8 and colony formation assays indicated that circCSPP1 significantly increased colon cancer cell proliferation, which was reversed by transfection with miR-431 mimics or by ROCK1 knockdown (Fig. 4B and C). Consistently, the Transwell assay results revealed that circCSPP1 notably promoted the migration and invasion of colon cancer cells, whereas these effects were reversed by miR-431 mimics or by ROCK1 knockdown (Fig. 4D and E). Additionally, the effects of circCSPP1, sh-ROCK1 or sh-ZEB1 on their target genes in cells were detected with RT-qPCR, respectively (Fig. S4A, B and C). Meanwhile, miR-431 mimics significantly increased the level of miR-431, while miR-431 inhibitor exhibited completely opposite effect (Fig. S4D and F). Taken together, these findings demonstrated that the knockdown of ROCK1 reversed the tumor-promoting effects of circCSPP1.

miR-431 targets ZEB1 in colon cancer cells. The present study then explored the interaction among circCSPP1, miR-431 and ZEB1. The potential complementary pairing sequence between miR-431 and the 3′-UTR of ZEB1 is presented in Fig. 5A. The results of luciferase reporter experiment indicated that miR-431 mimics significantly reduced the luciferase activity of cells carrying the WT ZEB1 3′-UTR (Fig. 5B). In addition, the results of RT-qPCR and western blot analyses revealed that miR-431 mimics notably decreased ZEB1 expression at the mRNA and protein level in the cells; by contrast, miR-431 inhibitor increased ZEB1 expression (Fig. 5C-E). Moreover, RIP assay using the antibody against Ago2 confirmed the interaction between miR-431 and ZEB1 (Fig. 5F).

Subsequently, the interaction between circCSPP1 and ZEB1 was investigated using RT-qPCR. The data revealed that the overexpression of circCSPP1 promoted the level of ZEB1; however, this phenomenon was completely reversed by transfection with miR-431 mimics or by ZEB1 knockdown (Fig. 5G). Similarly, the promoting effects of circCSPP1 on cell invasion and migration were significantly inhibited by ZEB1 knockdown (Fig. 5H and I). Thus, these data illustrated miR-431 targeted ZEB1 in colon cancer cells.

circCSPP1 activates the cyclin D1/CDK4/Rb signaling pathway in colon cancer. To further examine the role of the circCSPP1 in colon cancer, the levels of cell cycle-related proteins were detected using western blot analysis. The results indicated that the overexpression of circCSPP1 increased the expression of ROCK1, cyclin D1, p-CDK4 and p-Rb in the cells; however, these phenomena were reversed by transfection with miR-431 mimics or by ROCK1 knockdown (Fig. 6A). Moreover, it was found that circCSPP1 overexpression also increased the expression of ZEB1 and Snail, and downregulated the E-cadherin level. Similarly, the effects of circCSPP1 overexpression on these proteins were reversed by transfection with miR-431 mimics or by ZEB1 knockdown (Fig. 6B). In addition, circCSPP1 knockdown induced G1 arrest, while circCSPP1 overexpression promoted G1 arrest in colon cancer cells (Fig. S3A and B). The potential mechanism through which circCSPP1 regulates the progression of colon cancer are presented in Fig. 6C. The schematic diagram illustrates that circCSPP1 promotes the progression of colon cancer by regulating the miR-431/ROCK1 and miR-431/ZEB1 pathways.

Transfer of circCSPP1 from SW620 cells to macrophages cells via exosomes. As is known, tumor-derived exosomes play vital roles in cancer progression (27). Therefore, in the present study, exosomes were isolated from SW620 cells (with or without circCSPP1 overexpression). As demonstrated in Fig. 7A and B, the tumor cell-derived exosomes were round, cup-shaped particles ranging from 50 to 150 nm in diameter. In addition, the exosomal protein markers, CD81 and CD9, were highly expressed in the exosomes derived from the SW620 cells (Fig. 7C). Moreover, the level of circCSPP1 in exosomes derived from the SW620 cells overexpressing circCSPP1 was significantly unregulated compared with that from the control SW620 cells (Fig. 7D).

To explore cell-to-cell crosstalk by transmitting circCSPP1 between SW620 cells and macrophages (PMA-stimulated THP-1 monocytes), macrophages were incubated with SW620 cell-derived exosomes (PKH26-labeled) for 48 h. The results indicated that the PKH26 lipid dye could be observed in the cytoplasm of the macrophages, suggesting that the SW620 cell-derived exosomes were transferred to the macrophages (Fig. 7E). On the whole, these data suggested circCSPP1 could be transferred from SW620 cells to macrophages via exosomes.

SW620 cell-derived exosomes promote macrophage M2 polarization. The present study then examined the effects of exosomes derived from SW620 cells (with or without circCSPP1 overexpression) on macrophage M2 polarization. As demonstrated in Fig. 8A, exosomes derived from SW620 cells (with or without circCSPP1 overexpression) significantly increased the rate of CD206-positive macrophages. In addition, the levels of the M2 macrophage-associated cytokines, arginase-1 and IL-10, were significantly increased when the macrophages incubated with exosomes derived from SW620 cells (with or without circCSPP1 overexpression) (Fig. 8B). Moreover, the invasiveness and migratory ability of the SW620 cells was notably promoted when the cells were co-incubated with exosome-treated macrophages (Fig. 8C). These data suggested that SW620 cell-derived exosomes promoted macrophage M2 polarization.

Discussion

Increasing evidence has uncovered the critical role of circRNAs in the progression of human cancers, including colon cancer (19, 20). A previous study reported that circCCDC66 expression was upregulated in colon cancer and a high expression of circCCDC66 was associated with a poor prognosis of the patients (28). In the present study, the dysregulated circRNAs were analyzed using the GEO database. A novel circRNA back-splicing 8-11 exons of the CSPP1 gene, termed circCSPP1, was found, which plays a tumor-promoting role in colon cancer.

Subsequently, the mechanisms through which circCSPP1 regulates the progression of colon cancer were explored. circRNA can function as a sponge of various miRNAs and as a competing endogenous RNA. In colon cancer, hsa_circ_0055625 has been shown to increase cell proliferation by sponging miR-106b-5p (1). circRNA CBL.11 has been shown to suppress cell proliferation by sponging miR-6778-5p (29). Similar to these reports, the present study found that circCSPP1 promoted the progression of colon cancer by sponging miR-431 and regulating the expression of ROCK1 and ZEB1.

ROCK1/2 are Rho-GTPase effectors that control vital aspects of the actin cytoskeleton. The RhoA/ROCK pathway is activated in a variety of tumors and exerts a direct regulatory effect on the mobility of tumor cells (30–32). Previous research has indicated that G1/S progression requires ROCK (33). The role of ROCK1 in the regulation of the cell cycle may explain its effect on the proliferation of colon cancer cells. The other pathway is the induction of CDKI p16, which prevents the CDK4/6-mediated phosphorylation of Rb proteins, thereby blocking E2F-dependent transcription (34). The present study found that circCSPP1 promoted the expression of cyclin D1, p-CDK4 and p-Rb through the regulation of ROCK1 and miR-431. In addition, ZEB1 is well-known to be involved in the regulation of EMT in cancer cells (35). The present study found that circCSPP1 promoted EMT in colon cancer by modulating ZEB1. However, there are more experiments are required to explore the possible interaction between miR-431/ROCK1 and miR-431/ZEB1. Such as can inhibition of one or more signaling pathways in Figure 6C attenuate the growth, migration and invasion of the cancer cells, even with circCSPP1 overexpression? In addition, one limitation of current study is that circCSPP1/miR-431/ROCK1/Cyclin D/Rb axis was validated and the complex of cyclin D1 and CDK4 was not explored yet.

It has been reported that tumor cell-derived exosomes are closely associated with the progression of cancer (36), since exosomes can improve the microenvironment of cancer cells (37). Moreover, M2 macrophages have been reported to promote tumor metastasis and recurrence (38). In the present study, SW620 cell-derived exosomes increased M2 macrophage polarization, which in turn promoted the migration and invasion of colon cancer cells. However, a potential limitation of current study is that the properties of macrophage were not analyzed in the *in vivo* xenograft models.

In conclusion, the findings of the present study demonstrated that circCSPP1 was upregulated in colon cancer and functioned as an oncogene. In addition, circCSPP1 promoted the progression of colon cancer functions as a competing endogenous RNA by the regulating miR-431/ROCK1 and miR-431/ZEB1 pathways. It was also found that circCSPP1 could be transferred from SW620 cells to macrophages via

exosomes and, thus, enhanced the microenvironment of colon cancer. The findings presented herein may provide novel insight into the pathogenesis of colon cancer.

Declarations

Acknowledgements

This study was supported by grants from the National Science Foundation of China (NSFC, no. 31770985, no. 82073180). Jiangsu Provincial Key Research and Development Program, China (no. BE2019665). Jiangsu Provincial Medical Youth Talent, China (no. QNRC2016732). Suzhou Municipal Project of Gusu Health Talent, Young Top Talent, China (no. 2018-057). Gusu Health Talents Cultivation Program, China (no. GSWS2019028). Scientific Research Program of Jiangsu Provincial “333 Projects”, China (no. BRA2019327). Science and Technology Program of Suzhou City, China (no. SYS2019053, no. SLC201906).

Availability of data and materials

The datasets used and/or analyzed during the current study are available from the corresponding author on reasonable request.

Ethics approval and consent to participate

This study was approved by the First Affiliated Hospital of Soochow University Ethical Committee (approval no. 2019834). All animal housing and experiments were conducted in strict accordance with the Institutional Guidelines for Care and Use of Laboratory Animals.

Conflict of interests

These authors declared no competing interests in this research.

References

1. Zhang J, Liu H, Zhao P, Zhou H, Mao T. Has_circ_0055625 from circRNA profile increases colon cancer cell growth by sponging miR-106b-5p. Journal of cellular biochemistry. 2019;120:3027–37.
2. Wang L, Peng X, Lu X, Wei Q, Chen M, Liu L. Inhibition of hsa_circ_0001313 (circCCDC66) induction enhances the radio-sensitivity of colon cancer cells via tumor suppressor miR-338-3p: Effects of cicr_0001313 on colon cancer radio-sensitivity. Pathol Res Pract. 2019;215:689–96.
3. Feng J, Ma J, Liu S, Wang J, Chen Y. A noncoding RNA LINC00504 interacts with c-Myc to regulate tumor metabolism in colon cancer. J Cell Biochem, 2019.

4. Zhang X, Liu H, Sun B, Sun Y, Zhong W, Liu Y, Chen S, Ling H, Zhou L, Jing X, et al. Novel Podophyllotoxin Derivatives as Partial PPARgamma Agonists and their Effects on Insulin Resistance and Type 2 Diabetes. Sci Rep. 2016;6:37323.
5. Miller KD, Nogueira L, Mariotto AB, Rowland JH, Yabroff KR, Alfano CM, Jemal A, Kramer JL, Siegel RL. Cancer treatment and survivorship statistics, 2019. Cancer J Clin. 2019;69:363–85.
6. Miller KD, Nogueira L, Mariotto AB, Rowland JH and Clinicians RLSJCACJf: Cancer treatment and survivorship statistics, 2019. 2019.
7. Zhong W, Chen S, Zhang Q, Xiao T, Qin Y, Gu J, Sun B, Liu Y, Jing X, Hu X, et al. Doxycycline directly targets PAR1 to suppress tumor progression. Oncotarget. 2017;8:16829–42.
8. Yang S, Zhang H, Guo L, Zhao Y, Chen F. Reconstructing the coding and non-coding RNA regulatory networks of miRNAs and mRNAs in breast cancer. Gene. 2014;548:6–13.
9. Siciliano V, Garzilli I, Fracassi C, Criscuolo S, Ventre S and di Bernardo D: MiRNAs confer phenotypic robustness to gene networks by suppressing biological noise. Nat Commun 4: 2364, 2013.
10. Zhang B, Pan X, Cobb GP, Anderson TA. microRNAs as oncogenes and tumor suppressors. Developmental biology. 2007;302:1–12.
11. Liu B, Shyr Y, Cai J, Liu Q. Interplay between miRNAs and host genes and their role in cancer. Brief Funct Genomics. 2018;18:255–66.
12. Chen Q, Liu T, Bao Y, Zhao T, Wang J, Wang H, Wang A, Gan X, Wu Z, Wang L. CircRNA cRAPGEF5 inhibits the growth and metastasis of renal cell carcinoma via the miR-27a-3p/TXNIP pathway. Cancer Lett. 2020;469:68–77.
13. Wei S, Zheng Y, Jiang Y, Li X, Geng J, Shen Y, Li Q, Wang X, Zhao C, Chen Y, et al. The circRNA circPTPRA suppresses epithelial-mesenchymal transitioning and metastasis of NSCLC cells by sponging miR-96-5p. EBioMedicine. 2019;44:182–93.
14. Song T, Xu A, Zhang Z, Gao F, Zhao L, Chen X, Gao J, Kong X. CircRNA hsa_circRNA_101996 increases cervical cancer proliferation and invasion through activating TPX2 expression by restraining miR-8075. J Cell Physiol. 2019;234:14296–305.
15. Zhong W, Liu P, Zhang Q, Li D, Lin J. Structure-based QSAR, molecule design and bioassays of protease-activated receptor 1 inhibitors. J Biomol Struct Dyn. 2017;35:2853–67.
16. Zhao J, Xia H, Wu Y, Lu L, Cheng C, Sun J, Xiang Q, Bian T, Liu Q. CircRNA_0026344 via miR-21 is involved in cigarette smoke-induced autophagy and apoptosis of alveolar epithelial cells in emphysema. Cell Biol Toxicol, 2021.
17. Guo Z, Xie M, Zou Y, Liang Q, Liu F, Su J, He Z, Cai X, Chen Z, Zhao Q, et al. Circular RNA Hsa_circ_0006766 targets microRNA miR-4739 to regulate osteogenic differentiation of human bone marrow mesenchymal stem cells. Bioengineered. 2021;12:5679–87.
18. Li X, Ding J, Wang X, Cheng Z, Zhu Q. NUDT21 regulates circRNA cyclization and ceRNA crosstalk in hepatocellular carcinoma. Oncogene, 2019.
19. Verduci L, Strano S, Yarden Y, Blandino G. The circRNA-microRNA code: emerging implications for cancer diagnosis and treatment. Molecular oncology. 2019;13:669–80.

20. Yu J, Yang M, Zhou B, Luo J, Zhang Z, Zhang W, Yan Z: CircRNA-104718 acts as competing endogenous RNA and promotes hepatocellular carcinoma progression through microRNA-218-5p/TXNDC5 signaling pathway. Clinical science (London, England: 1979) 133: 1487-1503, 2019.
21. Livak KJ, Schmittgen TD. Analysis of relative gene expression data using real-time quantitative PCR and the 2(-Delta Delta C(T)) Method. Methods. 2001;25:402–8.
22. Meng J, Ai X, Lei Y, Zhong W, Qian B, Qiao K, Wang X, Zhou B, Wang H, Huai L, et al. USP5 promotes epithelial-mesenchymal transition by stabilizing SLUG in hepatocellular carcinoma. Theranostics. 2019;9:573–87.
23. Zhong W, Yang W, Qin Y, Gu W, Xue Y, Tang Y, Xu H, Wang H, Zhang C, Wang C, et al: 6-Gingerol stabilized the p-VEGFR2/VE-cadherin/beta-catenin/actin complex promotes microvessel normalization and suppresses tumor progression. J Exp Clin Cancer Res 38: 285, 2019.
24. Zheng X, Huang M, Xing L, Yang R, Wang X, Jiang R, Zhang L, Chen J. The circRNA circSEPT9 mediated by E2F1 and EIF4A3 facilitates the carcinogenesis and development of triple-negative breast cancer. Mol Cancer. 2020;19:73.
25. Zhong W, Sun B, Gao W, Qin Y, Zhang H, Huai L, Tang Y, Liang Y, He L, Zhang X, et al. Salvianolic acid A targeting the transgelin-actin complex to enhance vasoconstriction. EBioMedicine. 2018;37:246–58.
26. Wang Y, Sun J, Ma C, Gao W, Song B, Xue H, Chen W, Chen X, Zhang Y, Shao Q, et al. Reduced Expression of Galectin-9 Contributes to a Poor Outcome in Colon Cancer by Inhibiting NK Cell Chemotaxis Partially through the Rho/ROCK1 Signaling Pathway. PloS one. 2016;11:e0152599.
27. Whiteside TL. Tumor-Derived Exosomes and Their Role in Cancer Progression. Advances in clinical chemistry 74: 103–141, 2016.
28. Hsiao KY, Lin YC, Gupta SK, Chang N, Yen L, Sun HS, Tsai SJ. Noncoding Effects of Circular RNA CCDC66 Promote Colon Cancer Growth and Metastasis. Cancer research. 2017;77:2339–50.
29. Li H, Jin X, Liu B, Zhang P, Chen W, Li Q. CircRNA CBL.11 suppresses cell proliferation by sponging miR-6778-5p in colorectal cancer. BMC Cancer. 2019;19:826.
30. Huang GX, Wang Y, Su J, Zhou P, Li B, Yin LJ, Lu J. Up-regulation of Rho-associated kinase 1/2 by glucocorticoids promotes migration, invasion and metastasis of melanoma. Cancer Lett. 2017;410:1–11.
31. Tang Y, He Y, Zhang P, Wang J, Fan C, Yang L, Xiong F, Zhang S, Gong Z, Nie S, et al. LncRNAs regulate the cytoskeleton and related Rho/ROCK signaling in cancer metastasis. Mol Cancer. 2018;17:77.
32. Olson MF. Contraction reaction: mechanical regulation of Rho GTPase. Trends Cell Biol. 2004;14:111–4.
33. Kim H, Kang M, Lee SA, Kwak TK, Jung O, Lee HJ, Kim SH, Lee JW. TM4SF5 accelerates G1/S phase progression via cytosolic p27Kip1 expression and RhoA activity. Biochim Biophys Acta. 2010;1803:975–82.
34. Luh FY, Archer SJ, Domaille PJ, Smith BO, Owen D, Brotherton DH, Raine AR, Xu X, Brizuela L, Brenner SL, et al. Structure of the cyclin-dependent kinase inhibitor p19Ink4d. Nature. 1997;389:999–1003.

35. Lee SY, Jeong EK, Ju MK, Jeon HM, Kim MY, Kim CH, Park HG, Han SI, Kang HS. Induction of metastasis, cancer stem cell phenotype, and oncogenic metabolism in cancer cells by ionizing radiation. Mol Cancer. 2017;16:10.
36. Zeng Y, Fu BM. Resistance Mechanisms of Anti-angiogenic Therapy and Exosomes-Mediated Revascularization in Cancer. Front Cell Dev Biol. 2020;8:610661.
37. Yeon M, Lee S, Lee JE, Jung HS, Kim Y, Jeoung D. CAGE-miR-140-5p-Wnt1 Axis Regulates Autophagic Flux, Tumorigenic Potential of Mouse Colon Cancer Cells and Cellular Interactions Mediated by Exosomes. Front Oncol. 2019;9:1240.
38. Cheng W, Hao CY, Zhao S, Zhang LL, Liu D. SNHG16 promotes the progression of osteoarthritis through activating microRNA-93-5p/CCND1 axis. Eur Rev Med Pharmacol Sci. 2019;23:9222–9.

Figures

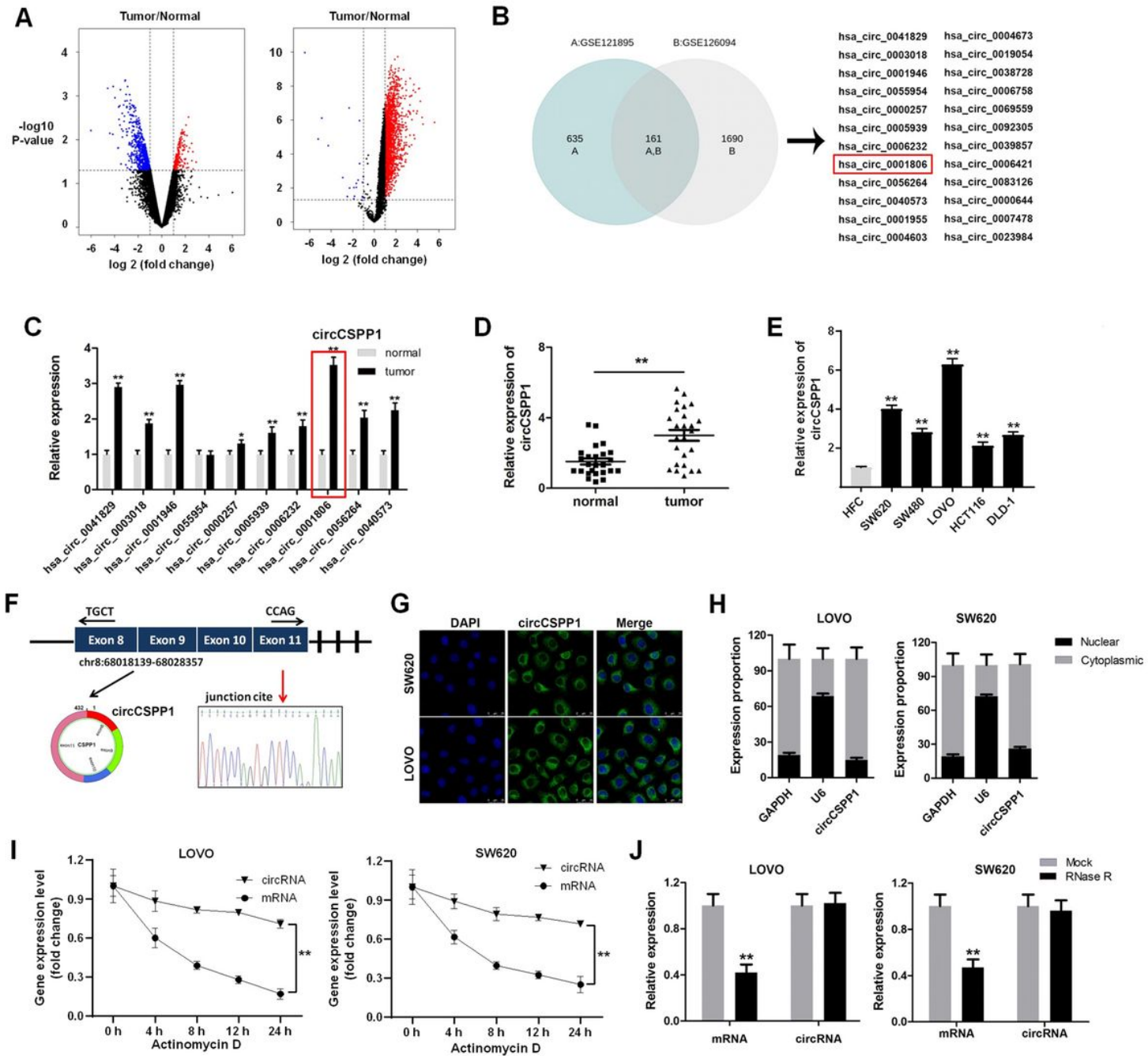

Figure 1

CircCSPP1 is highly expressed in colon cancer tissues.

(A) GEO database data analysis of colon cancer differentially expressed circRNA. **(B)** Wayne analysis of commonly differentially expressed circRNA in GSE121895 and GSE126094. **(C)** The expression of circRNAs in tumor tissues and in adjacent normal tissue was detected with RT-qPCR. **(D)** The expression of circCSPP1 in tumor tissues and in adjacent normal tissue was detected with RT-qPCR. **(E)** The expression of circCSPP1 in cell lines was tested with RT-qPCR. **(F)**The circRNA circularization mechanism is formed by splicing of exons 8 and 9, and sequencing confirmed the sequence is correct. **(G)** The localization of circCSPP1 in colon cancer cells was detected with FISH. **(H)** The expression of circCSPP1 in the nucleus and cytoplasm was detected by RT-qPCR. **(I)** The half-live of linear and circRNA were

detected by RT-qPCR, after actinomycin treatment. (J) The expression of linear and circRNA linear was detected with RT-qPCR, after RNase R treatment. *p<0.05 vs normal, **p<0.01 vs normal, HFC, mock groups; n = 3.

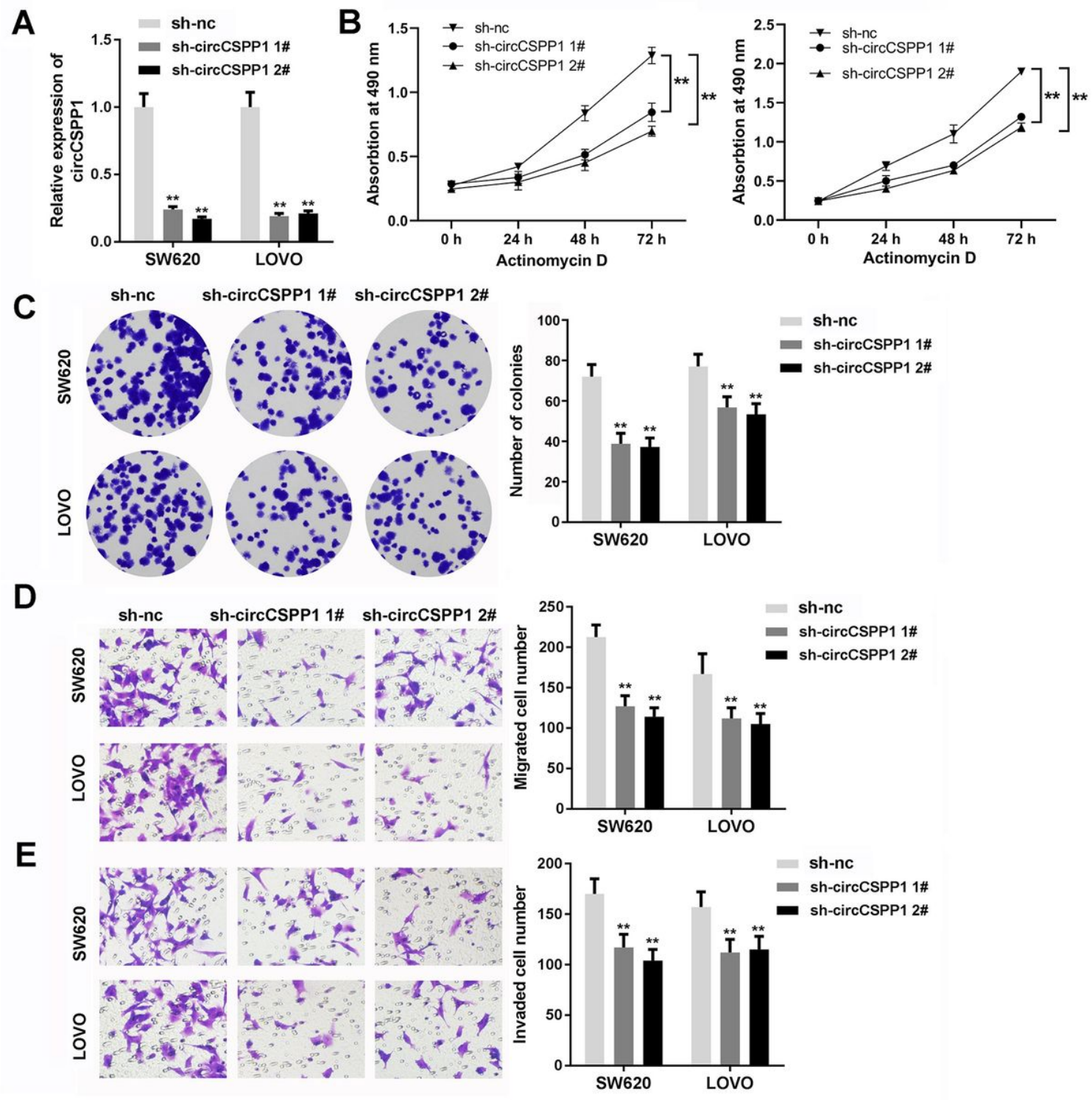

Figure 2

Knockdown of circCSPP1 significantly inhibits the tumorgenesis of colon cancer.

Colon cancer cells were treated with circCSPP1 shRNAs or negative control (sh-nc) for 24 h. **(A)** The expression of circCSPP1 was detected with RT-qPRC. **(B)** CCK8 was used to detect the viability of colon cancer cells. **(C)** Cell clone formation was used to assess the proliferation of clone cancer cells. **(D, E)** The cell migration and invasion ability was detected with transwell assay. **p<0.01 vs sh-nc; n = 3.

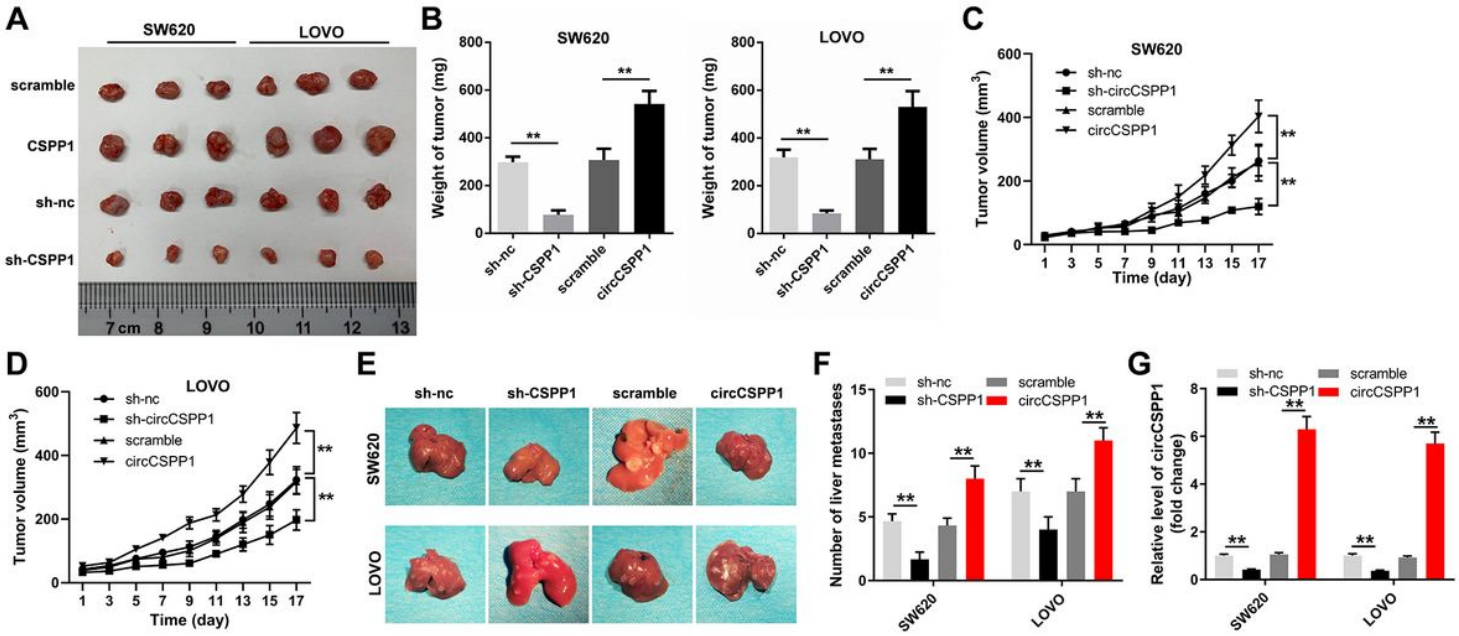

Figure 3

CircCSPP1 promotes colon cancer tumor growth and metastasis *in vivo*.

(A) Tumor volume in each group was imaged in the end of animal study. **(B)** The tumors in mice was isolated and weighted. **(C, D)** The tumor volumes of SW620 or LOVO tumor-bearing mice were monitored every two days. **(E, F)** Liver metastasis of colon cancer in the nude mice in each group was monitored and quantified. (**G**) The expression of circCSPP1 in tumor tissues was detected with RT-qPCR. **p<0.01; n = 6. PcDNA3.1 control (scramble).

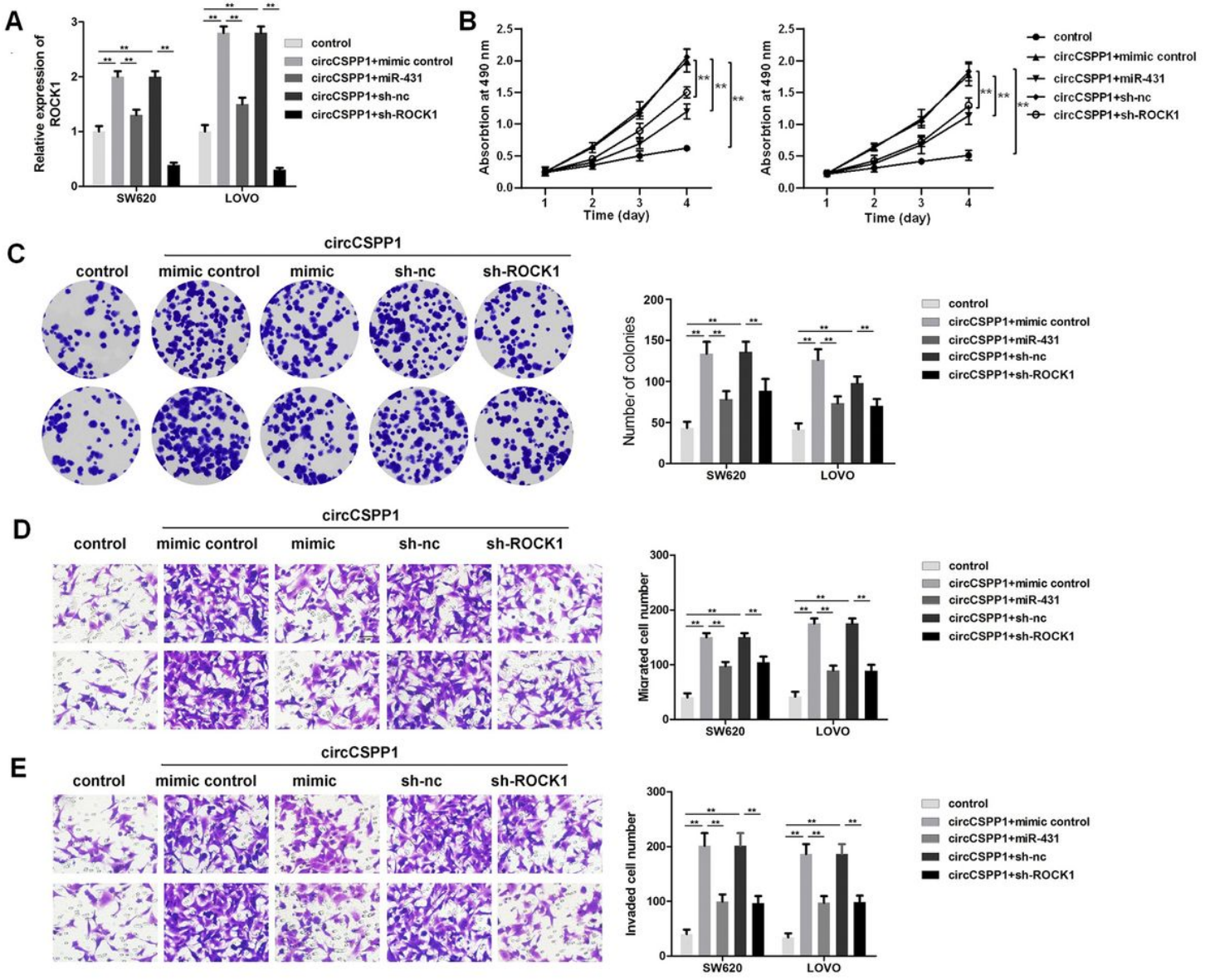

Figure 4

Knockdown of ROCK1 reverses the tumor-promoting effect of circCSPP1.

Colon cancer cells were treated with pcDNA3.1-circCSPP1, pcDNA3.1-circCSPP1 plus miR-431 mimics or pcDNA3.1-circCSPP1 plus ROCK1 shRNA. **(A)** The expression of ROCK1 was detected with RT-qPCR. **(B)** CCK8 was used to detect the cell viability in each group. **(C)** Cell clone formation was used to assess the proliferation of clone cancer cells. **(D, E)** Cell migration and invasion were detected with transwell assays. **p<0.01; n = 3.

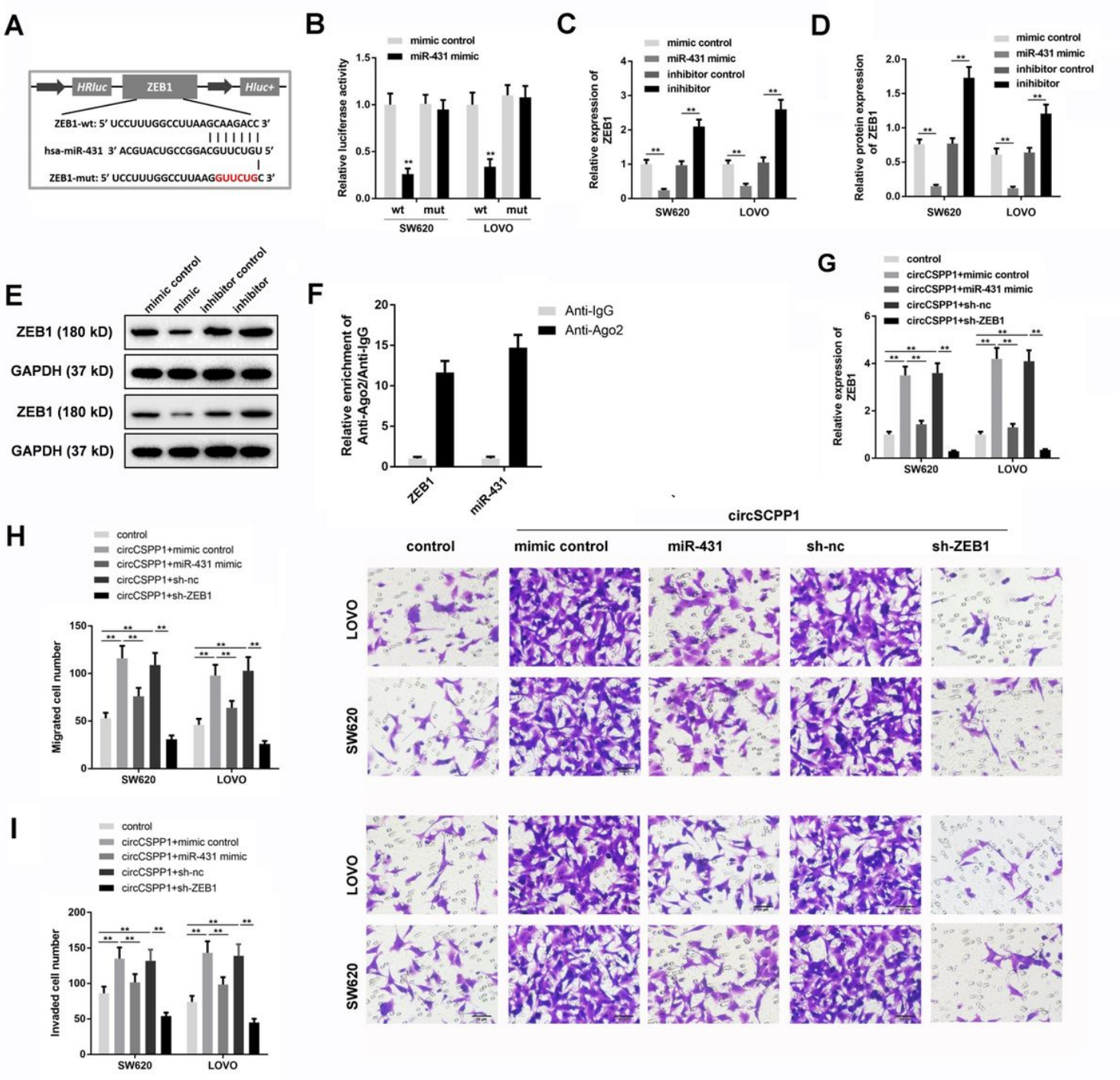

Figure 5

MiR-431 targets ZEB1 in colon cancer cells.

(A) The binding site between miR-431 and ROCK1 was predicted. **(B)** Luciferase reporter experiment was performed to detect the interaction between miR-431 and ZEB1. **(C, D and E)** colon cancer cells were treated with miR-431 mimics or miR-431 inhibitor for 24 h, the gene and protein level of ZEB1 was detected with RT-qPCR and WB, respectively. **(F)** RIP assay was performed to verify the binding between ZEB1 and miR-431. Colon cancer cells were treated with pcDNA3.1-circCSPP1, pcDNA3.1-circCSPP1 plus miR-431 mimics or pcDNA3.1-circCSPP1 plus ZEB1 shRNA **(G)**. RT-qPCR was used to detect the

expression of ZEB1. **(H, I)** Transwell assay was performed to assess the migration and invasion of colon cancer cells. **p<0.01; n = 3.

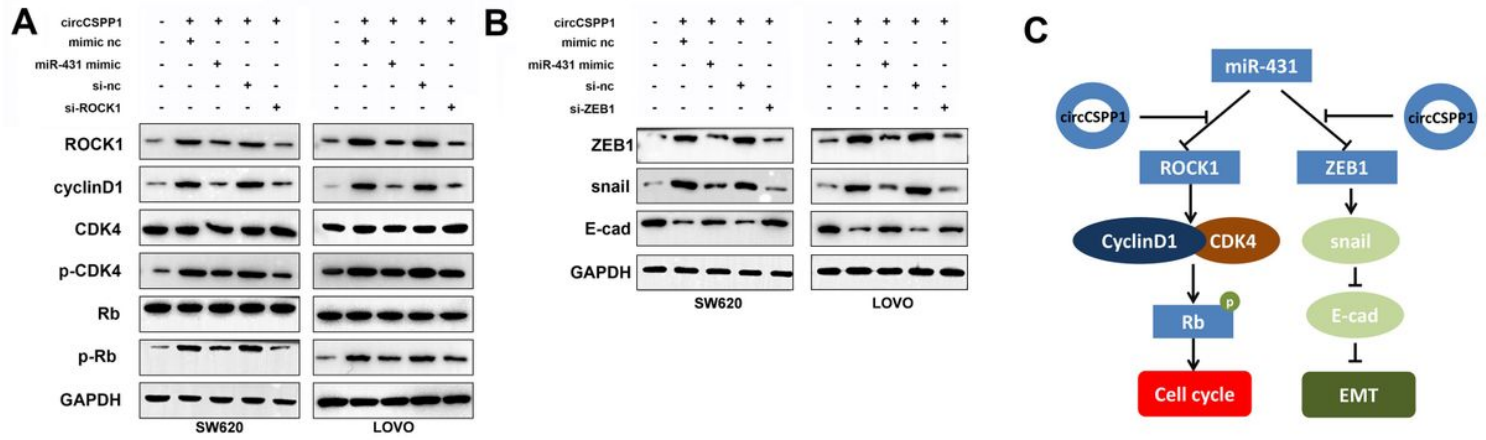

Figure 6

CircCSPP1 upregulates cyclin D1/CDK4/RB signaling pathway in colon cancer.

Colon cancer cells were treated with pcDNA3.1-circCSPP1, pcDNA3.1-circCSPP1 plus miR-431 mimics or pcDNA3.1-circCSPP1 plus ROCK1 shRNA. **(A, B)** Western blot was used to detect the expressions of cell cycle-related proteins (cyclin D1, CDK4, Rb) and EMT related protein (Snail, E-cadherin) in each group. **(C)** The potential mechanism by which circCSPP1 regulated the progression of colon cancer was presented. N = 3.

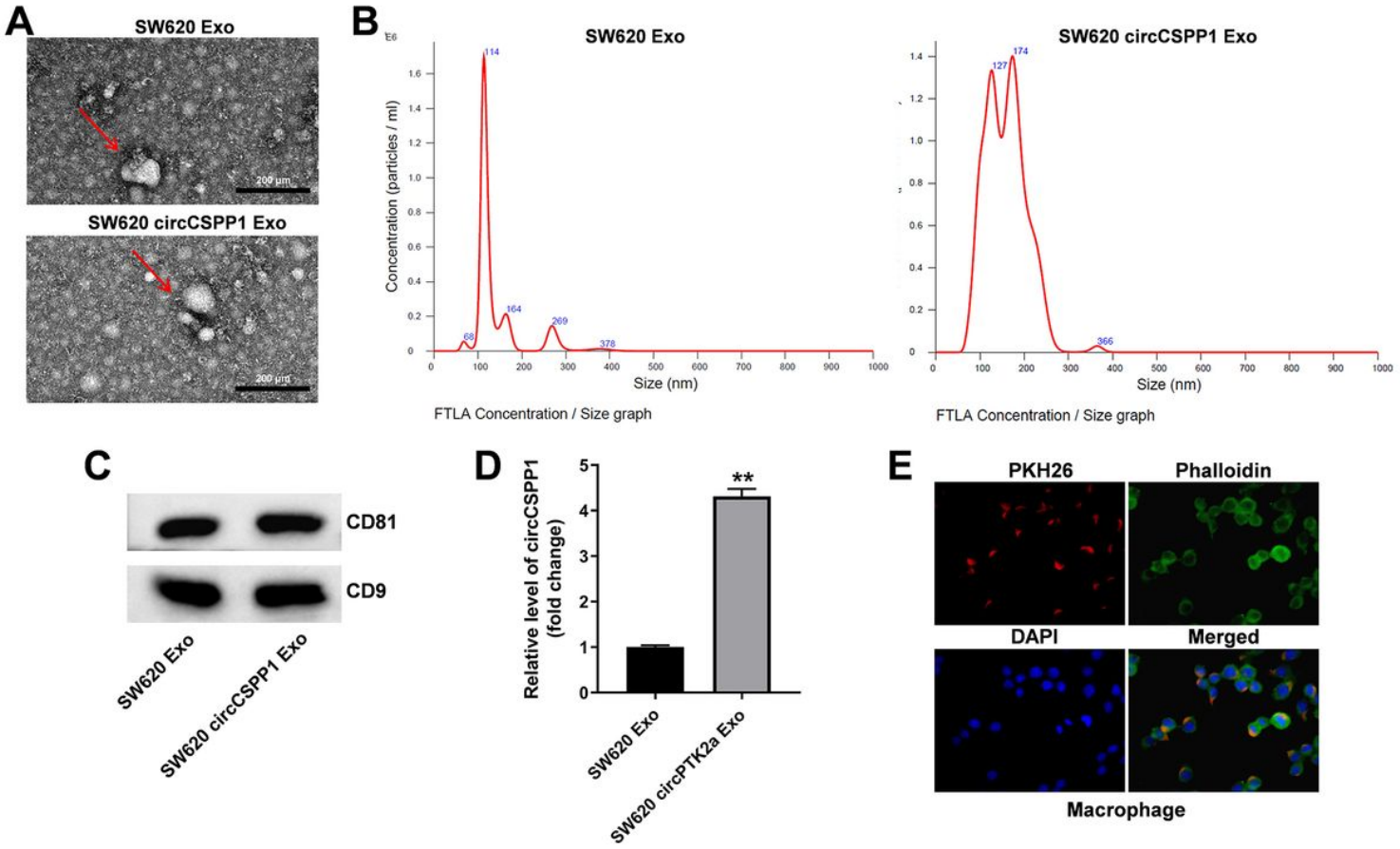

Figure 7

Isolation and characterization of exosomes.

(A) The morphology of isolated exosomes was observed by TEM. **(B)** The particle distribution of exosomes isolated from SW620 with or without pcDNA3.1-circCSPP1 (SW620 circCSPP1 Exo; SW620-Exo) was measured by NANOSIGHT. **(C)** The expressions of CD81 and CD9 in SW620-Exo or in SW620 circCSPP1 Exo were detected with western blot. **(D)** The level of -circCSPP1 in SW620-Exo or in SW620 circCSPP1 Exo was evaluated by RT-qPCR. **(E)** THP-1 (PMA-treated) cells were incubated with SW620-Exo for 24 h. Then, the cells dyed with PHK26, Phalloidin and DAPI and the morphology of cells was observed with fluorescence microscope. **p<0.01 compared with SW620-Exo; n = 3.

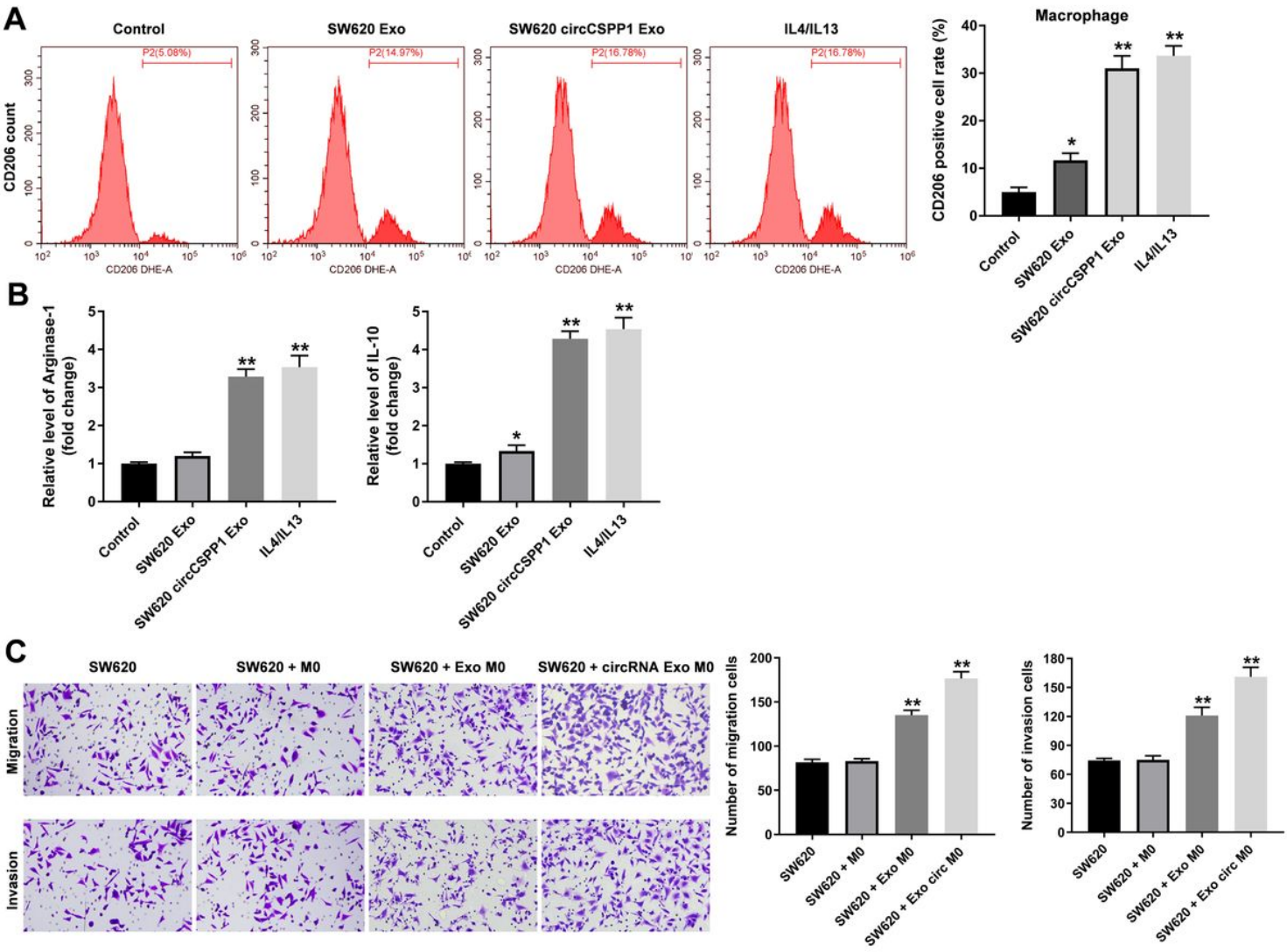

Figure 8

CircCSPP1 was transferred from SW620 cells to macrophages cells via exosomes.

Macrophages were cultured with SW620 Exo, SW620 circCSPP1 Exo or 20 ng/ml IL-4/IL-13 for 24 h. **(A)** The CD206 positive macrophages were measured and quantified by flow cytometry. **(B)** The levels of Arginase-1 and IL-10 in macrophages were evaluated with RT-qPCR. **(C)** SW620 cells were co-cultured with macrophages (M0), Exo-treated macrophages or circCSPP1 Exo treated macrophages for 24 h, the cell migration and invasion ability was detected with transwell assays. **p<0.01 compared with SW620; n = 3.

Supplementary Files

This is a list of supplementary files associated with this preprint. Click to download.

- FigureS1.jpg
- FigureS2.jpg
- FigureS3.jpg

- FigureS4.jpg